BIOCHEMISTRY
including biophysical chemistry & molecular biology

Article

pubs.acs.org/biochemistry

Structural Characterization of the Cyclic Cystine Ladder Motif of θ-Defensins

Anne C. Conibear,[†] K. Johan Rosengren,[†,‡] Peta J. Harvey,[†] and David J. Craik*[,†]

[†]Division of Chemistry and Structural Biology, Institute for Molecular Bioscience, The University of Queensland, Brisbane, QLD 4072, Australia

[‡]School of Biomedical Sciences, The University of Queensland, Brisbane, QLD 4072, Australia

Supporting Information

ABSTRACT: The θ-defensins are, to date, the only known ribosomally synthesized cyclic peptides in mammals, and they have promising antimicrobial bioactivities. The characteristic structural motif of the θ-defensins is the cyclic cystine ladder, comprising a cyclic peptide backbone and three parallel disulfide bonds. In contrast to the cyclic cystine knot, which characterizes the plant cyclotides, the cyclic cystine ladder has not been as well described as a structural motif. Here we report the solution structures and nuclear magnetic resonance relaxation properties in aqueous solution of three representative θ-defensins from different species. Our data suggest that the θ-defensins are more rigid and structurally defined than previously thought. In addition, all three θ-defensins were found to self-associate in aqueous solution in a concentration-dependent and reversible manner, a property that might have a role in their mechanism of action. The structural definition of the θ-defensins and the cyclic cystine ladder will help to guide exploitation of these molecules as structural frameworks for the design of peptide drugs.

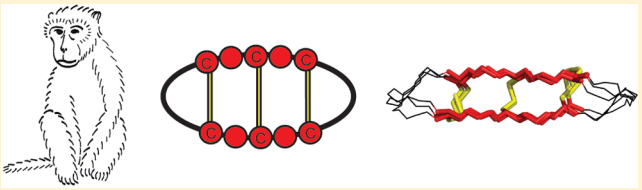

The first cyclic peptide to be discovered in mammals, rhesus θ-defensin-1 (RTD-1),[1] was isolated from the leukocytes of rhesus macaques and comprises an 18-residue cyclic backbone braced by three disulfide bonds, as shown in Figure 1. Although the θ-defensins are, to date, the only known cyclic peptides in mammals,[2] many backbone cyclic peptides have been isolated from bacteria, fungi, and plants.[3] The known cyclic peptides have been recently reviewed and include the bacteriocins, cyanobactins, and pilins from bacteria,[4] the amanita toxins from fungi,[5] and the caryophyllaceae-type peptides,[6] cyclotides,[7] sunflower trypsin inhibitors (SFTIs),[8,9] and squash trypsin inhibitors[10] from plants. The cyclotides share common features with the θ-defensins in that they have a cyclic peptide backbone and three disulfide bonds. The major structural difference is that the disulfide bonds in cyclotides are arranged in a cyclic cystine knot (CCK),[11] whereas the θ-defensins have their three disulfide bonds arranged in a cyclic cystine ladder (CCL) motif (Figure 1).[12] θ-Defensins are thought to be involved in innate immunity and have antibacterial, antifungal, and antiviral activities.[1] Interest has been shown in their use as topical antimicrobial agents because of their resistance to digestion by proteases in biological fluids and low hemolytic and cytotoxic activity.[13]

θ-Defensins are the only known cyclic peptides that are assembled from two separate gene products called demidefensins.[1] The two demidefensins are spliced together such that two nine-residue fragments are linked in a head-to-tail fashion through the formation of two new peptide bonds, resulting in the 18-residue cyclic θ-defensin, as illustrated in Figure 1, but very little is known about the biosynthetic mechanism behind this processing. Pairs of demidefensins may be spliced together in different combinations, as either homo- or heterodimers, resulting in a diversity of peptides encoded by the same genes.[14] Whereas RTD-1 is an example of a heterodimer, the baboon θ-defensin-2 (BTD-2), isolated from olive baboons (*Papio anubis*),[15] is a homodimer and so displays a 2-fold symmetry in its sequence.

Demidefensin genes have been identified in several primate species, including humans, and have highly conserved sequences.[16] However, not all demidefensin genes give rise to demidefensin peptides; the presence of a stop codon in the signal sequence of some demidefensin transcripts means that translation is prematurely terminated. Cole and co-workers discovered two such pseudogenes in humans and then synthesized the θ-defensins encoded by the pseudogenes and termed them "retrocyclins".[17] The heterodimeric θ-defensin, retrocyclin-2 [HTD-2 (Figure 1)], was found to have anti-HIV activity at nanomolar concentrations and is currently being developed as a topical microbicide.[13,17]

Only two structures of θ-defensins (RTD-1, in its cyclic and linear forms,[18] and HTD-2[12]) have been reported to date. As with the cyclotides, NMR has proven to be a useful method for determining the structure of θ-defensins because of their small size, solubility, and stability.[19,20] The reported structure of RTD-1 suggested surprising flexibility in solution given that the constrained cyclic backbone and three disulfide bonds form,

Received: October 5, 2012
Revised: November 12, 2012
Published: November 13, 2012

dx.doi.org/10.1021/bi301363a | *Biochemistry* 2012, 51, 9718−9726

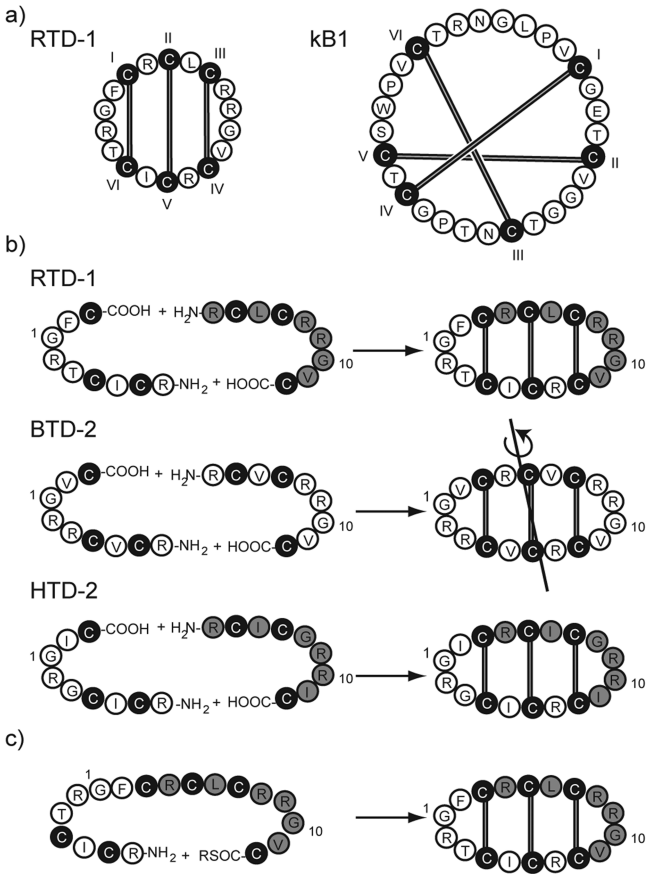

Figure 1. Sequences and disulfide arrangement of θ-defensins. (a) The three disulfide bonds in θ-defensins, illustrated for RTD-1, are I–VI, II–V, and III–IV connections, forming a cyclic cystine ladder (CCL) motif. The cyclotides have three disulfide bonds (I–IV, II–V, and III–VI), forming a cyclic cystine knot (CCK), as shown for kalata B1 (kB1). (b) θ-Defensins are biosynthesized from two precursors, resulting in the head-to-tail ligation of two nine-residue demidefensins to form an 18-residue cyclic peptide. RTD-1 and HTD-2 are heterodimers, biosynthesized from two different demidefensins (gray and white circles), whereas BTD-2 is a homodimer. The 2-fold sequence symmetry of BTD-2, coupled with the cyclic backbone, results in 2-fold rotational symmetry of the structure. Residues 1 and 10 are numbered, and the axis of symmetry of BTD-2 is shown. (c) The θ-defensins in this study were synthesized by solid phase peptide synthesis as a single linear peptide, and cyclization was achieved by native chemical ligation using a thioester linker, as shown for RTD-1. Amino acid residues are represented by their one-letter code, and sequences are written in a clockwise direction from the N- to C-terminus. Cysteine residues are colored black, and disulfide bonds are represented by gray bars.

essentially, four fused rings.[18] The structural flexibility was attributed to "bending" motions of the θ-defensin along its longitudinal axis, although the two turns appeared to be well-defined. The structure of HTD-2 was determined in the presence of sodium dodecyl sulfate (SDS) micelles and was found to be similar to that of RTD-1 but with less flexibility.[12] Ultracentrifugation and translational diffusion experiments indicated that HTD-2 self-associates as trimers at millimolar concentrations, and a model was proposed in which the monomers align longitudinally, with the disulfide bonds facing inward, based on selective resonance broadening of the cystine residues in the NMR data.

The ease of synthesis,[21,22] the stability, and the great diversity of cyclic peptides make them suitable for a wide range of applications, based on their intrinsic bioactivities and their potential as drug scaffolds for bioactive peptides.[23,24] Several methods, including both chemical[1,25] and recombinant,[26] have been developed for the synthesis of θ-defensins, but only two structures have been reported. Knowledge of the three-dimensional structure of cyclic peptides is crucial for grafting and design applications because it provides structures for modeling simulations and information about structure–activity relationships. In addition, potential applications of θ-defensins as drug scaffolds or probes for investigating β-sheet protein–protein interactions will be facilitated by the availability of structures of a range of different θ-defensins. The characterization of the cyclic cystine ladder as a structural motif and an understanding of how different sequences affect its structural and dynamic properties will aid its development as a structural framework for peptide drugs.

The purpose of this study was to characterize the cyclic cystine ladder structural motif by determining the high-resolution NMR solution structures of a representative set of θ-defensins: the prototype θ-defensin, RTD-1, the first symmetrical θ-defensin, BTD-2, and a retrocyclin, HTD-2. Improved NMR and structure calculation methods have become available since the publication of the first θ-defensin structures, and this study describes the effects of these methods and the use of information from heteronuclear NMR experiments on the RTD-1 and HTD-2 structures as well as reporting the novel structure of BTD-2. The flexibility and self-associative behavior of the θ-defensins were also investigated to give insights into their possible mechanism of action.

MATERIALS AND METHODS

Peptide Synthesis. The θ-defensins RTD-1, BTD-2, and HTD-2 were synthesized on a 0.5 mmol scale by manual solid phase peptide synthesis (SPPS) using *tert*-butyloxycarbonyl (Boc) chemistry. Boc-protected amino acids were purchased from Novabiochem or GL Biochem (Shanghai, China) with standard side chain protecting groups: Arg(Tos), Cys(4-MeBzl), and Thr(Bzl). The peptide chain was assembled on Boc-Gly-phenylacetamidomethyl resin (Boc-Gly-PAM resin) (Novabiochem) via a thioester linker generated by removal of the Boc group with trifluoroacetic acid (TFA) and coupling of *S*-trityl-β-mercaptopropionic acid to the resin, followed by removal of the trityl group with a TFA/triisopropylsilane (TIPS)/water mixture (96:2:2). Boc-protected amino acids were double coupled using activation with 2-(1*H*-benzotriazol-1-yl)-1,1,3,3-tetramethyluronoium hexafluorophosphate (HBTU) or 2-(6-chloro-1*H*-benzotriazol-1-yl)-1,1,3,3-tetramethylaminium hexafluorophosphate (HCTU) and neutralized in situ with diisopropylethylamine (DIPEA) in dimethylformamide (DMF). The coupling efficiency was monitored by the quantitative ninhydrin reaction.[27]

The θ-defensins were synthesized from the C- to N-terminus, with the starting point for synthesis chosen to give an N-terminal cysteine residue (Cys14 for RTD-1 and BTD-2 and Cys5 for HTD-2) to allow cyclization by native chemical ligation.[28] After removal of the final N-terminal Boc group with TFA, the resin was washed with DMF and dichloromethane and dried under nitrogen. The peptide was cleaved from the resin with an HF/*p*-cresol/*p*-thiocresol mixture (20:1:1, v:v:v) at 0 °C for 2 h. Residual HF was removed by evaporation, and the peptide was precipitated with cold diethyl ether, dissolved

dx.doi.org/10.1021/bi301363a | *Biochemistry* 2012, 51, 9718–9726

in a 50% acetonitrile/water mixture, and lyophilized. Crude purification was conducted by RP-HPLC using a 1%/min gradient of 90% acetonitrile in 0.05% aqueous TFA on a preparative C_{18} column (Phenomenex). Electrospray mass spectrometry (ES-MS) was used to confirm the mass and purity of the peptides. Cyclization by native chemical ligation[28] and oxidation were conducted concurrently in NH_4HCO_3 buffer (0.1 M, pH 8.5) overnight. The cyclic peptides were then further purified by RP-HPLC using a 0.5%/min gradient of 90% acetonitrile in 0.05% aqueous TFA with absorbance detection at 215 nm and lyophilized.

NMR Spectroscopy. Peptide samples for ^1H, ^{13}C, and ^{15}N NMR measurements were prepared in either a 90% H_2O/10% D_2O mixture or 99.96% D_2O (Cambridge Isotope Laboratories) at ~1 mM and pH ~4 (uncorrected for isotope effects). The concentrations of the peptide solutions were determined by comparison of the intensities of the RP-HPLC trace with that of a standard quantified by amino acid analysis.[29] Chemical shifts were referenced internally to sodium 2,2-dimethyl-2-silapentane-5-sulfonate (DSS). Spectra were recorded on Bruker Avance-500, Bruker Avance-600, or Bruker Avance-900 spectrometers at 298 K, or 283−308 K for variable-temperature experiments. All two-dimensional (2D) spectra were recorded in phase-sensitive mode using time-proportional phase incrementation for quadrature detection in the t_1 dimension.[30] Water suppression was achieved using excitation sculpting with gradients.[31] The 2D experiments included TOCSY[32] using a MLEV-17 spin lock sequence with a 80 ms mixing time, NOESY[33] with a 150 or 300 ms mixing time, DQF-COSY,[34] ECOSY,[35] ^{13}C HSQC,[36] and ^{15}N HSQC[36] experiments. Spectra were acquired with 4096 data points in the F_2 dimension and 512 increments in the F_1 dimension. The t_1 dimension was zero-filled to 1024 real data points, and the F_1 and F_2 dimensions were multiplied by a sine-squared function prior to Fourier transformation. $^3J_{HN-H\alpha}$ coupling constants were measured from one-dimensional (1D) spectra or from antiphase cross-peak splitting in the DQF-COSY spectrum, and $^3J_{H\alpha-H\beta}$ coupling constants were measured from the ECOSY spectrum and, together with intraresidual NOE intensities, were used for stereospecific assignments.[37] Spectra were processed with TopSpin (Bruker) and assigned with CCPNMR[38] using the sequential assignment protocol.[39]

Amide protons involved in intramolecular hydrogen bonds were identified by their slow exchange after the dissolution of the peptide in 99.96% D_2O and the sensitivity of the amide proton chemical shift to temperature. Temperature coefficients at pH ~4 were calculated from series of TOCSY spectra acquired at 283−308 K, and amide protons with temperature coefficients more positive than −4.6 ppb/K were considered to be involved in intramolecuar hydrogen bonding interactions.[40] Amide proton cross-peaks detected in the TOCSY spectra >4 h after dissolution in D_2O at 298 K were classified as slowly exchanging.

Pulse field gradient NMR diffusion experiments were used to measure the translational diffusion coefficients of the θ-defensins relative to dioxane (3 μL of a 1% solution in D_2O) as an internal standard.[41] Diffusion experiments were performed with a 2D sequence using stimulated echo longitudinal encode-decode.[42] The lengths of all pulses and delays were held constant, and 64 spectra were acquired, with the strength of the diffusion gradient varying between 2 and 95% of the maximal value. The lengths of the diffusion gradient and the stimulated echo were optimized for each sample to give a total decay in the protein signal of ~90%. The data were analyzed using the T1 processing method in Topspin (Bruker). Comparison with dioxane (effective hydrodynamic radius of 2.12 Å) allowed the effective hydrodynamic radii of the θ-defensins to be calculated, and the radii were then used to estimate the number of residues in the aggregate.[43] Errors in the hydrodynamic radii were calculated as the standard deviation over seven or eight signals. The dependence of the association state on peptide concentration was determined by performing diffusion experiments at peptide concentrations between 0.5 and 4 mM for each of the RTD-1, BTD-2, and HTD-2 peptides. Stepwise dilution of the 4 mM solutions to 0.5 mM established the reversibility of the self-association.

The $^1H-^{13}C$ NOE on:off ratios were obtained from 2D $^1H-^{13}C$ correlation spectra via double inept transfer using sensitivity improvement with decoupling during acquisition. NOE on and NOE off experiments were interleaved and then split prior to Fourier transformation with a zero scaling factor. The two spectra were phased identically, and the intensities of the respective peaks were determined using CCPNMR. Experiments were performed in triplicate on a single sample, and errors were calculated as the standard deviation over the three experiments.

Structure Calculations. Interproton distance restraints were derived from the intensity of cross-peaks in NOESY spectra recorded with a mixing time of 300 ms at 298 K. A list of interproton distances was generated from the chemical shifts and NOE intensities using the CALIBA function in CYANA-3.0.[44] For the symmetrical peptide BTD-2, only residues 5−13 were assigned and the distance restraints were subsequently duplicated for the corresponding residues 1−4 and 14−18. Pseudoatom corrections were applied to nonstereospecifically assigned protons. Structure calculations were then performed without automated assignment using the CALC function in CYANA-3.0. Restraints for the cyclic peptide bond, disulfide bonds, hydrogen bonds, and dihedral angles were added.

Constraints for the ϕ and ψ backbone dihedral angles were generated using TALOS[45,46] from the Hα, Cα, Cβ, HN, and N chemical shifts. The predicted angle ranges were checked for consistency with coupling constant information from the 1D spectra and NOE peak intensities in a 150 ms NOESY spectrum.[37] Residues having a $^3J_{HN-H\alpha}$ of ≤5 Hz were expected to have a predicted ϕ angle of $-60 \pm 30°$, and residues with a $^3J_{HN-H\alpha}$ of ≥8 Hz were expected to have a predicted ϕ angle of $-120 \pm 30°$. Side chain χ^1 angles and stereospecific assignments of methylene pairs that could be deduced from the $^3J_{H\alpha-H\beta}$ coupling constants and Hα−HN sequential NOE peak intensities were included in the angle restraints. Disulfide bond restraints were included, based on the cystine ladder arrangement of the disulfide bonds in RTD-1,[1,18] with disulfide bond connectivities between residues 3 and 16, 5 and 14, and 7 and 12. Restraints for hydrogen bonding pairs were included for residues with amide protons that were slowly exchanging and had temperature coefficients more positive than −4.6 ppb/K.[40]

The CALC function in CYANA[44] was used to perform 10000 steps of torsion angle dynamics and generate an ensemble of 50 initial structures from which the 20 lowest-energy structures were chosen for analysis. Several rounds of structure calculations were performed to resolve restraint violations. Protocols from the RECOORD database[47] were then used to calculate an ensemble of 50 structures within CNS,[48] using the force field distributed with Haddock 2.0.[49]

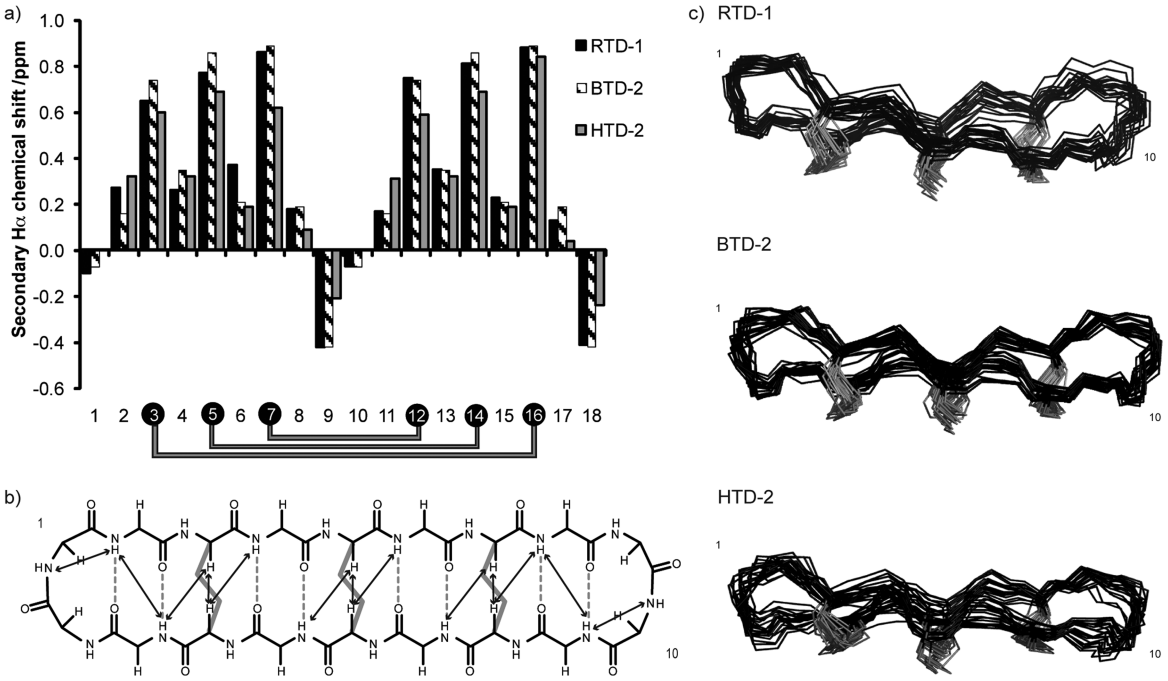

Figure 2. Structural comparison of θ-defensins RTD-1, BTD-2, and HTD-2. (a) Secondary Hα chemical shifts of the θ-defensins show a well-defined β-sheet structure comprising residues 2−8 and 11−17 joined by two turns comprising residues 9 and 10 and residues 18 and 1. The cysteine residues are colored black, and the disulfide connectivities are indicated by gray bars. (b) Hydrogen bonding and inter-residue NOE interactions (shown for RTD-1) support the β-sheet and turn structure and were included as restraints in the structure calculations. Hydrogen bonds are shown as gray dashed lines, inter-residue NOE interactions as black arrows, and disulfide bonds as gray bars. (c) Three-dimensional NMR solution structures of RTD-1, BTD-2, and HTD-2 show well-defined β-sheet structures braced by three disulfide bonds. For each peptide, an ensemble of the 20 minimum-energy structures is shown in line format with the backbone colored black and the disulfide bonds colored gray. Residues 1 and 10 are indicated.

The torsion angle simulated annealing protocol includes a high-temperature phase of 5000 steps at 10000 K followed by a cooling phase to 1000 K over 5000 steps and a second cooling phase from 1000 to 50 K over 5000 steps (all with 3 fs time steps). The 50 structures generated were then further refined in a water shell.[50] Each peptide was subjected to (i) slow heating from 100 to 500 K in 100 K temperature steps, each comprising 200 steps of Cartesian dynamics using a time step of 3 fs (during this phase, the harmonic position restraints for the heavy atoms are in place but slowly phased out); (ii) refinement at 500 K through 2000 Cartesian dynamics steps (4 fs time steps); (iii) slow cooling from 500 to 25 K in 25 K steps, each comprising 2000 Cartesian dynamics steps (4 fs time steps); and (iv) final minimization with 200 steps of Powell minimization. A final set of 20 structures with the lowest energy and no violations greater than 0.2 Å or 2° was selected for analysis using MolProbity.[51] The structures were visualized using MOLMOL,[52] and figures were generated using PyMOL.

RESULTS

The synthesis of RTD-1, BTD-2, and HTD-2 proceeded smoothly by Boc SPPS, followed by concurrent oxidation and cyclization by native chemical ligation in ammonium bicarbonate (0.1 M, pH 8.5, overnight), as shown in Figure 1c. Preliminary analyses of the reaction by liquid chromatography and mass spectrometry (Figure S1 of the Supporting Information) indicated that cyclization occurs within 15 min of addition to the ammonium bicarbonate solution and is followed by a stepwise oxidation to form three disulfide bonds over approximately 8 h. The desired three-disulfide isomer was the major product, and NMR analysis supported the predicted cyclic backbone and cystine ladder arrangement of the disulfide bonds. The peptides were soluble in water at a concentration of approximately 1 mM (pH ∼3.5) and remained stable in solution. At higher pH, the solubility of the θ-defensins is significantly reduced. The signals in the TOCSY spectra were generally well dispersed, although some spin systems in HTD-2 were overlapped. Sequential Hα−HN cross-peaks in the NOESY spectra confirmed the unbroken cyclic backbone.

The secondary Hα shifts of the three θ-defensins (RTD-1, BTD-2, and HTD-2) in water are shown in Figure 2a and indicate that the peptides adopt a well-defined β-sheet structure joined by two turns. Secondary proton chemical shifts are calculated as the difference between the chemical shift of each proton in the peptides and the published "random coil shift" of that proton.[53] The magnitude of the secondary Hα shift indicates the deviation of the peptide structure from an unstructured random coil, and its sign can be used to predict the secondary structure: β-strand (positive) or α-helix/turn (negative).[53] Comparison of the secondary Hα shifts shows that the three peptides adopt similar structures comprising extended antiparallel β-strand regions between residues 2 and 8 and residues 11 and 17 joined by turns made up of residues 9 and 10 and residues 18 and 1. The secondary Hα shifts also agree with those reported for RTD-1 in 10% acetonitrile[18] or 20 mM $NaPO_4$ buffer[25,26] and HTD-2[12] in 100 mM SDS, respectively.

The cross-strand NOE interactions observed in the 2D spectra are consistent with the predicted antiparallel β-strand structure and are illustrated in Figure 2b. In addition to distance restraints generated from the NOE intensities, inclusion of hydrogen bonding and dihedral angle constraints in the

dx.doi.org/10.1021/bi301363a | Biochemistry 2012, 51, 9718−9726

Table 1. Structural Statistics for RTD-1, BTD-2, and HTD-2

	RTD-1	BTD-2	HTD-2
NMR and Refinement Statistics			
no. of distance and dihedral constraints			
total NOE	107	72	117
intraresidue	63	28	45
inter-residue	44	44	72
sequential ($\|i - j\| = 1$)	34	30	59
medium-range ($\|i - j\| \leq 4$)	4	8	3
long-range ($\|i - j\| \geq 5$)	6	6	10
no. of hydrogen bond restraints[a]	8	8	4
no. of disulfide bond restraints	3	3	3
total no. of dihedral angle restraints	36	42	37
ϕ	15	17	16
ψ	15	17	15
χ^1	6	8	6
mean NOE violations >0.0	0.55	0.65	0.00
mean NOE violations >0.2	0	0	0
mean dihedral violations >0	4.1	3.5	0.6
mean dihedral violations >2	0	0	0
Structural Statistics[b]			
rmsd from mean structure (Å)			
backbone atoms	0.68 ± 0.23	0.77 ± 0.29	1.02 ± 0.39
heavy atoms	1.80 ± 0.31	2.07 ± 0.49	2.62 ± 0.55
stereochemical quality[c]			
Ramachandran favored (%)	100 ± 0	100 ± 0	89.4 ± 4.6
Ramachandran outliers (%)	0 ± 0	0 ± 0	1.6 ± 2.8
unfavorable side chain rotamers (%)	0.31 ± 1.40	0 ± 0	1.00 ± 2.44
Clashscore, all atoms[d]	2.66 ± 2.27	2.31 ± 2.88	3.43 ± 3.41
percentile	97.0 ± 4.0	96.5 ± 7.4	94.0 ± 6.7
overall MolProbity score	0.98 ± 0.33	0.86 ± 0.34	1.58 ± 0.42
percentile	99.2 ± 0.9	99.2 ± 1.4	88.0 ± 11.1

[a]Two restraints were used per hydrogen bond. [b]Statistics are given as means ± the standard deviation. [c]According to MolProbity (http://molprobity.biochem.duke.edu). [d]Defined as the number of steric overlaps of >0.4 Å per 1000 atoms.

structure calculations resulted in well-defined structures consistent with the large secondary α-shifts. Residues taking part in hydrogen bonding interactions were identified by their temperature coefficients and by deuterium exchange experiments. Amide protons with temperature coefficients more positive than −4.6 ppb/K are regarded as being shielded from the solvent and likely to be involved in hydrogen bonding interactions.[40] The amide protons of residues 2, 4, 6, 8, 11, 13, 15, and 17 showed temperature insensitivity in all three peptides, suggesting the presence of four hydrogen bond pairs across the β-strand as shown in Figure 2b. The slow exchange of the amide protons listed above with deuterium, on dissolution of the lyophilized peptide in D_2O, provided further evidence of the presence of the predicted hydrogen bond pairs. Dihedral angle restraints for the backbone ϕ and ψ angles were obtained from the angles predicted by TALOS using the Hα, Cα, Cβ, HN, and N chemical shifts.[45,46]

For each of the θ-defensins (RTD-1, BTD-2, and HTD-2), an ensemble of 20 minimum-energy structures was selected from the structures calculated and refined in a water shell using CNS, and the structural statistics are summarized in Table 1. The well-defined antiparallel β-strands comprising residues 2−8 and 11−17 are connected by two type βI′ turns, as shown in Figure 2c, resulting in a slight twist of the β-sheet. The positive ϕ and ψ angle predictions from TALOS for residues 9, 10, 18, and 1 were only included as restraints in the structure calculations after confirmation from initial structures using only the NOE-derived distance restraints. Strong 8Hα−9HN and relatively weak 9NH−9Hα NOE cross-peaks provided additional evidence of the positive ϕ and ψ angles of the turn residues. The glycine residue in position $i + 2$, which is required for β'-turns, is conserved in all known θ-defensins except for HTD-2.

The 20 minimum-energy structures selected from the CNS refinement were analyzed in Molprobity,[51] and the results are summarized in Table 1. The RTD-1, BTD-2, and HTD-2 structures have been deposited in the Protein Data Bank as entries 2lyf for RTD-1, 2lye for BTD-2, and 2lzi for HTD-2, and the chemical shifts have been deposited at the BioMagResBank as entries 18723 for RTD-1, 18722 for BTD-2, and 18757 for HTD-2.

To confirm that the higher structural definition obtained in the θ-defensin structure calculations was characteristic of the cyclic cystine ladder and not simply due to inclusion of excessive restraints, ^{1}H−^{13}C NOE data were acquired as an indication of the flexibility of the molecule. Heteronuclear NOE on:off ratios of the Cα−Hα bonds were calculated for each of the residues and are shown in Figure 3a. The ^{13}C NMR relaxation parameters T_1, T_2, and NOE are dependent on the overall and internal motions of a protein and can be used to determine the rates and amplitudes of these motions.[54,55] The observed NOE on:off ratios (Figure 3a) are all between 1.2 and 1.5, with the exception of those of residues 9, 10, and 18 of HTD-2. The observed NOE on:off ratios indicate that overall

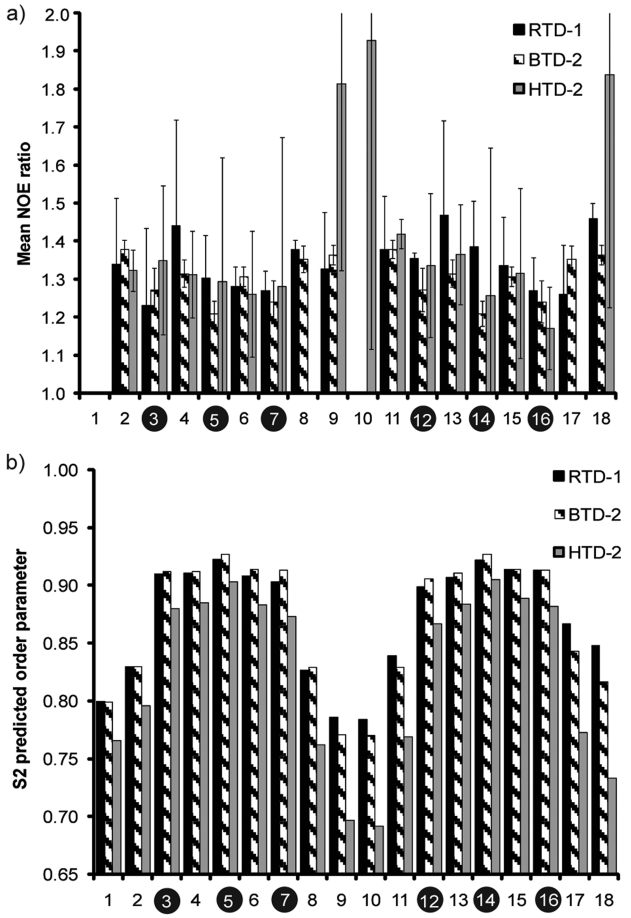

Figure 3. Heteronuclear NOE ratios and predicted S^2 order parameters showing the rigidity of the cyclic cystine ladder structure. (a) $^1H-^{13}C$ NOE ratios for Cα–Hα cross-peaks for each residue in RTD-1, BTD-2, and HTD-2. Error bars are shown as the standard deviation over three experiments. (b) S^2 order parameters for each residue in RTD-1, BTD-2, and HTD-2, as predicted by TALOS using the Hα, Cα, Cβ, NH, and N chemical shifts. Cysteine residues are colored black.

motion is on the nanosecond time scale and that all the residues have similar internal motion.[55] An alternative measure of the internal motion of a residue relative to the rest of the protein is the generalized order parameter S^2, which ranges from zero for unrestricted motion to one for completely restricted motion.[55] Generalized order parameters (S^2) calculated within TALOS,[46] using the random coil index method,[56] were also compared across the three cyclic peptides and are shown in Figure 3b. The majority of the residues in the θ-defensins studied have predicted order parameters of >0.75, supporting the rigidity of the structures calculated from the NMR data. The relatively low order parameters for residues 9, 10, and 18 in HTD-2 agree with the high NOE on:off ratios of the same residues, indicating that the turns in HTD-2 are more flexible than those of RTD-1 and BTD-2. For all three peptides, the exceptionally high order parameters for residues 2–8 and 11–17 relative to the turns (residues 9 and 10 and residues 18 and 1) illustrate the structural definition and stability of the cyclic cystine ladder and suggest that the turns are more flexible than the center of the molecule.

Translational diffusion measurements and 1D spectra recorded at different peptide concentrations show that RTD-1, BTD-2, and HTD-2 self-associate in a concentration-dependent manner. In this study, broadening of the 1D proton spectra of RTD-1, BTD-2, and HTD-2 was observed as the peptide concentration increased, suggesting that self-association is a common feature of the θ-defensins. Figure 4 shows the self-association state of RTD-1, BTD-2, and HTD-2 as a function of concentration. In agreement with the published data, a trimeric aggregation state was obtained at a concentration of approximately 2.6 mM for HTD-2.[12] However, translational diffusion measurements at concentrations above and below 2.6 mM suggest that, for all three θ-defensins, the self-association is nonspecific and concentration-dependent. Significant broadening of the signals at high concentrations, however, results in large errors in the diffusion measurements at high concentrations, so the self-association might level off to five to six peptide units at concentrations of >4 mM. Dilution of the associated θ-defenisn samples resulted in a return to the monomeric state, showing that the self-association is reversible.

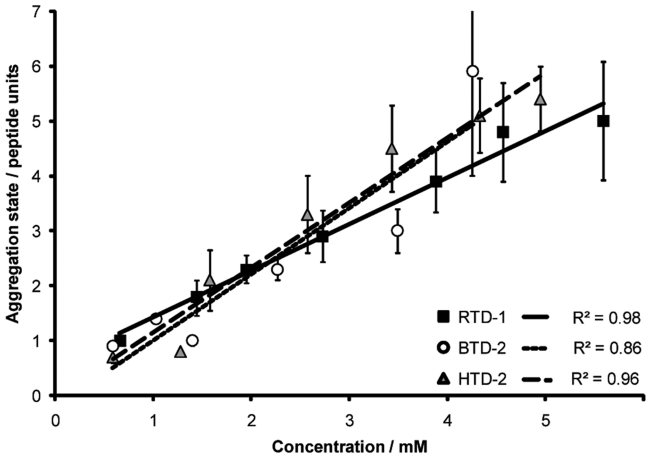

Figure 4. Aggregation state of RTD-1, BTD-2, and HTD-2 as a function of peptide concentration in D_2O. The number of peptide units was calculated from NMR translational diffusion measurements and shows an approximately linear relationship to the peptide concentration between 0.6 and 5.0 mM. Error bars are shown as the standard deviation over seven to eight signals in the spectra.

DISCUSSION

The synthetic strategy for θ-defensins involving concurrent oxidation and cyclization by native chemical ligation appears to be more efficient than previous syntheses involving a two-step process of oxidation followed by cyclization using peptide coupling methods.[1,18] The use of Boc-SPPS followed by native chemical ligation[57,58] has been widely used for the synthesis of cysteine-containing cyclic peptides but has not been described for θ-defensins. A recent report of a single-step cyclization and folding of RTD-1 using a sulfonamide safety-catch linker provides an alternative high-yielding strategy for the synthesis of θ-defensins using Fmoc chemistry.[25] Although isotope labeling of the θ-defensins was not necessary for their structure determination by NMR, the expression of θ-defensins in *Escherichia coli* has been reported[26] and could provide a method of producing isotope-labeled θ-defensins for further structural analysis. The ease of chemical synthesis of the θ-defensins, as described above, facilitates the determination of their structure by NMR and makes them a promising scaffold for peptide drugs. Formation of the cyclic cystine ladder as the major

dx.doi.org/10.1021/bi301363a | *Biochemistry* 2012, 51, 9718–9726

product during oxidation suggests the thermodynamic stability of the cyclic cystine ladder as a structural motif.

In contrast to the published θ-defensin structural studies,[12,18] in which acetonitrile was used as a cosolvent, NMR data for all three peptides were obtained in water, allowing direct comparison of the structures of the three θ-defensins. The secondary Hα shifts reported for RTD-1[18,25,26] and HTD-2[12] in aqueous solution agree with those shown in Figure 2a; however, the structural data reported were obtained in 10% aqueous acetonitrile and 100 mM SDS, respectively. In all three θ-defensins, the secondary Hα shifts for the six cysteine residues are particularly large, approaching 1 ppm, indicating the highly structured nature of the cyclic cystine ladder.

Only nine spin systems were present in the BTD-2 spectra, consistent with the findings that BTD-2 is biosynthesized as a homodimer of two demidefensin precursors[15] and, because of its cyclic backbone, exhibits molecular C_2 symmetry. The peak degeneracy arising from the 2-fold rotational symmetry in sequence indicates that the three-dimensional structure is also symmetrical about the center of rotation. Figure 1b illustrates the sequential and structural symmetry of BTD-2, a property that has also been observed for a bifunctional SFTI analogue.[59] The spectra of HTD-2 do not show degeneracy of all the residues, illustrating that a single-residue difference between the constituent demidefensins is sufficient to remove the structural symmetry.

The small size and solubility of the θ-defensins mean that ^{13}C and ^{15}N HSQC spectra can be acquired at natural abundance, providing additional chemical shift data for ϕ and ψ angle predictions using TALOS. The ^{15}N chemical shifts for RTD-1 obtained from HSQC spectra at natural abundance agree with those reported for the isotopically labeled peptide produced recombinantly.[26] The predicted ϕ and ψ angles were in agreement with the expected β-sheet structure, and their inclusion as restraints in the structure calculations resulted in considerable reduction in the backbone rmsd values, allowing us to precisely define the cyclic cystine ladder. In the proton spectra, the amide proton signals of residues 9 and 18 are broad and the amide cross-peak was not observed in the ^{15}N HSQC spectrum, suggesting that these residues might be in exchange between two conformations, which is consistent with the TALOS prediction of lower order parameters for these residues relative to the overall molecule. The residues comprising the tight turns and their three-dimensional conformations are important considerations in exploiting θ-defensins as templates for the design of peptide drugs.

The Clashscore, defined as the number of van der Waals overlaps (>0.4 Å) per 1000 atoms,[51] was initially high because of clashes between the α-protons of the disulfide-bonded cysteine residues. The constrained β-staple disulfide bond[60] forces the Cys Hα protons into proximity of each other; however, the van der Waals repulsions between the Hα protons force a slight adjustment of the disulfide bond conformation. Increasing the minimal distance restraint between the cysteine α-protons from 1.8 to 2.0 Å allowed the α-protons to be in proximity without van der Waals overlap.

The structures of the three representative θ-defensins (Figure 5a) define the cyclic cystine ladder structural motif (Figure 5b,c) and show that it is highly conserved within the θ-defensins. As expected, all three peptides have similar β-hairpin structures, consistent with the secondary Hα shifts, hydrogen bonding, and NOE data. In contrast to the published structures of RTD-1 and HTD-2, the ensembles obtained in this study

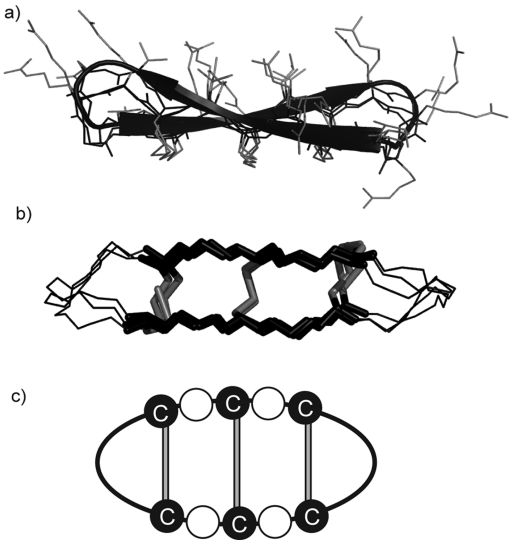

Figure 5. Structural definition of the cyclic cystine ladder motif. (a) Superimposed minimum-energy structures of RTD-1, BTD-2, and HTD-2. A cartoon representation of the RTD-1 secondary structure highlights the twisted antiparallel β-sheet. The three parallel disulfide bonds occupy one face of the molecule, and the side chains of the remaining residues are exposed on the other face. Backbone atoms are shown as black lines and side chains as gray lines. (b) Cyclic cystine ladder motif shown in stick representation to illustrate that the cyclic cystine ladder core is highly conserved over the three different primate species. (c) Diagrammatic representation illustrating how the cyclic cystine ladder could be applied as a stable core for the development of peptide drugs. White circles indicate how different amino acids could be used to impart desired bioactivities onto the framework. The black line represents how the turn regions could be expanded or modified.

have smaller rmsd values and improved Ramachandran analyses, indicating that the θ-defensins are more rigidly structured and less flexible than previously thought. The improved refinement statistics are mostly due to the additional hydrogen bonding and dihedral angle information available from the D_2O exchange and ^{13}C and ^{15}N HSQC experiments, respectively. Earlier structure calculations on RTD-1[18] and HTD-2[12] did not have access to the ^{13}C and ^{15}N HSQC information, leading to the suggestion that the θ-defensins were flexible. In our calculations that incorporated the ^{13}C and ^{15}N data, the backbone structures are well-defined, although the heavy-atom rmsd values are relatively high, suggesting that the side chains are flexible with respect to the backbone. The flexibility of the side chains exposed on one face of the β-sheet is characteristic of the cyclic cystine ladder motif (Figure 5a), in which the backbone is highly constrained by the cross-bracing disulfide and hydrogen bonds, leaving the side chains exposed to the solvent with limited interactions between the various side chains. The flexibility of the side chains is also supported by the observation that the peaks of the two Hβ protons in Arg4 and Arg8 overlap in the TOCSY spectra.

Self-association of HTD-2 in aqueous solution at concentrations of >0.6 mM was found using ultracentrifugation and NMR translational diffusion experiments and was proposed to contribute to its mechanism of action.[12] Our study supports the finding that HTD-2 self-associates as trimers at a concentration of 2.6 mM in water but shows that the number of θ-defensin units in the aggregate is concentration-dependent (Figure 4). The concentration-dependent self-association suggests that interactions between the θ-defensin molecules are nonspecific

because no particular multimer appears to be favored. Although the biological significance of self-association at concentrations of >1 mM is not clear, some α-defensins have been found at millimolar concentrations in vesicles.[61] High concentrations of θ-defensins might be present in phagosomes, and therefore, self-association could have a role in their antimicrobial activity. Alternatively, self-association in vesicles might aid packing and storage and keep the θ-defensins in an inactive form until they reach their site of action.

CONCLUSIONS

Three representative θ-defensins, RTD-1, BTD-2, and HTD-2, from different primate species have been successfully synthesized by solid phase peptide synthesis and cyclized using native chemical ligation. Structural characterization with improved NMR data and analysis methods has shown that the structures of RTD-1 and HTD-2 are rigid and well-defined and has demonstrated full structural symmetry of BTD-2. We have also shown that all three θ-defensins aggregate in a concentration-dependent and reversible manner. The structures are highly conserved among the θ-defensins and comprise an extended β-sheet region joined by two type βI′ turns. The characteristic feature of the θ-defensins is the cyclic cystine ladder structural motif comprising three parallel disulfide bonds joining two adjacent β-sheets. Definition of the cyclic cystine ladder of θ-defensins will facilitate its application as a stable core for the development of peptide-based drugs.

ASSOCIATED CONTENT

Supporting Information

Cyclization and oxidation of HTD-2 in 0.1 M NH_4HCO_3 at pH 8.5 (Figure S1). This material is available free of charge via the Internet at http://pubs.acs.org.

AUTHOR INFORMATION

Corresponding Author

*Institute for Molecular Bioscience, The University of Queensland, Brisbane, QLD 4072, Australia. E-mail: d.craik@imb.uq.edu.au. Phone: +61 (0)7 3346 2019.

Funding

Work in our laboratory on cyclic peptides is funded by the Australian Research Council (Grant DP0984390). D.J.C. is a National Health and Medical Research Council (NHMRC) Professorial Fellow (Grant APP1026501). K.J.R. is an NHMRC CDA Fellow (Grant APP631420).

Notes

The authors declare no competing financial interest.

ACKNOWLEDGMENTS

We thank Prof. Norelle Daly for helpful discussions and assistance with NMR assignments.

ABBREVIATIONS

NMR, nuclear magnetic resonance; HIV, human immunodeficiency virus; RTD-1, rhesus θ-defensin-1; BTD-2, baboon θ-defensin-2; HTD-2, human θ-defensin-2; HPLC, high-performance liquid chromatography; SDS, sodium dodecyl sulfate; CCK, cyclic cystine knot; CCL, cyclic cystine ladder; SFTI-1, sunflower trypsin inhibitor-1; rmsd, root-mean-square deviation; NOE, nuclear Overhauser enhancement.

REFERENCES

(1) Tang, Y.-Q., Yuan, J., Ösapay, G., Ösapay, K., Tran, D., Miller, C. J., Ouellette, A. J., and Selsted, M. E. (1999) A cyclic antimicrobial peptide produced in primate leukocytes by the ligation of two truncated α-defensins. *Science 286*, 498−502.

(2) Lehrer, R. I., Cole, A. M., and Selsted, M. E. (2012) θ-defensins: Cyclic peptides with endless potential. *J. Biol. Chem. 287*, 27014−27019.

(3) Craik, D. J. (2006) Seamless proteins tie up their loose ends. *Science 311*, 1563−1564.

(4) Montalbán-López, M., Sánchez-Hidalgo, M., Cebrián, R., and Maqueda, M. (2012) Discovering the bacterial circular proteins: Bacteriocins, cyanobactins, and pilins. *J. Biol. Chem. 287*, 27007−27013.

(5) Göransson, U., Burman, R., Gunasekera, S., Strömstedt, A. A., and Rosengren, K. J. (2012) Circular proteins from plants and fungi. *J. Biol. Chem. 287*, 27001−27006.

(6) Condie, J. A., Nowak, G., Reed, D. W., Balsevich, J. J., Reaney, M. J. T., Arnison, P. G., and Covello, P. S. (2011) The biosynthesis of caryophyllaceae-like cyclic peptides in *Saponaria vaccaria l.* From DNA-encoded precursors. *Plant J. 67*, 682−690.

(7) Saether, O., Craik, D. J., Campbell, I. D., Sletten, K., Juul, J., and Norman, D. G. (1995) Elucidation of the primary and three-dimensional structure of the uterotonic polypeptide kalata B1. *Biochemistry 34*, 4147−4158.

(8) Luckett, S., Garcia, R. S., Barker, J. J., Konarev, A. V., Shewry, P. R., Clarke, A. R., and Brady, R. L. (1999) High-resolution structure of a potent, cyclic proteinase inhibitor from sunflower seeds. *J. Mol. Biol. 290*, 525−533.

(9) Korsinczky, M. L., Schirra, H. J., and Craik, D. J. (2004) Sunflower trypsin inhibitor-1. *Curr. Protein Pept. Sci. 5*, 351−364.

(10) Chiche, L., Heitz, A., Gelly, J. C., Gracy, J., Chau, P. T., Ha, P. T., Hernandez, J. F., and Le-Nguyen, D. (2004) Squash inhibitors: From structural motifs to macrocyclic knottins. *Curr. Protein Pept. Sci. 5*, 341−349.

(11) Craik, D. J., Daly, N. L., Bond, T., and Waine, C. (1999) Plant cyclotides: A unique family of cyclic and knotted proteins that defines the cyclic cystine knot structural motif. *J. Mol. Biol. 294*, 1327−1336.

(12) Daly, N. L., Chen, Y. K., Rosengren, K. J., Marx, U. C., Phillips, M. L., Waring, A. J., Wang, W., Lehrer, R. I., and Craik, D. J. (2007) Retrocyclin-2: Structural analysis of a potent anti-HIV θ-defensin. *Biochemistry 46*, 9920−9928.

(13) Penberthy, W. T., Chari, S., Cole, A. L., and Cole, A. M. (2011) Retrocyclins and their activity against HIV-1. *Cell. Mol. Life Sci. 68*, 2231−2242.

(14) Leonova, L., Kokryakov, V. N., Aleshina, G., Hong, T., Nguyen, T., Zhao, C., Waring, A. J., and Lehrer, R. I. (2001) Circular minidefensins and posttranslational generation of molecular diversity. *J. Leukocyte Biol. 70*, 461−464.

(15) Garcia, A. E., Ösapay, G., Tran, P. A., Yuan, J., and Selsted, M. E. (2008) Isolation, synthesis, and antimicrobial activities of naturally occurring θ-defensin isoforms from baboon leukocytes. *Infect. Immun. 76*, 5883−5891.

(16) Nguyen, T. X., Cole, A. M., and Lehrer, R. I. (2003) Evolution of primate θ-defensins: A serpentine path to a sweet tooth. *Peptides 24*, 1647−1654.

(17) Cole, A. M., Hong, T., Boo, L. M., Nguyen, T., Zhao, C., Bristol, G., Zack, J. A., Waring, A. J., Yang, O. O., and Lehrer, R. I. (2002) Retrocyclin: A primate peptide that protects cells from infection by T- and M-tropic strains of HIV-1. *Proc. Natl. Acad. Sci. U.S.A. 99*, 1813−1818.

(18) Trabi, M., Schirra, H. J., and Craik, D. J. (2001) Three-dimensional structure of RTD-1, a cyclic antimicrobial defensin from rhesus macaque leukocytes. *Biochemistry 40*, 4211−4221.

(19) Craik, D. J., and Daly, N. L. (2007) NMR as a tool for elucidating the structures of circular and knotted proteins. *Mol. Biosyst. 3*, 257−265.

(20) Daly, N. L., Rosengren, K. J., Troeira Henriques, S., and Craik, D. J. (2011) NMR and protein structure in drug design: Application to cyclotides and conotoxins. *Eur. Biophys. J. 40*, 359−370.
(21) Conibear, A. C., and Craik, D. J. (2011) Chemical synthesis of naturally-occurring cyclic mini-proteins from plants and animals. *Isr. J. Chem. 51*, 908−916.
(22) Tam, J. P., and Wong, C. T. T. (2012) Chemical synthesis of circular proteins. *J. Biol. Chem. 287*, 27020−27025.
(23) Craik, D. J., Cemazar, M., and Daly, N. L. (2006) The cyclotides and related macrocyclic peptides as scaffolds in drug design. *Curr. Opin. Drug Discovery Dev. 9*, 251−260.
(24) Garcia, A. E., and Camarero, J. A. (2010) Biological activities of natural and engineered cyclotides, a novel molecular scaffold for peptide-based therapeutics. *Curr. Mol. Pharmacol. 3*, 153−163.
(25) Aboye, T. L., Li, Y. L., Majumder, S., Hao, J. F., Shekhtman, A., and Camarero, J. A. (2012) Efficient one-pot cyclization/folding of rhesus θ-defensin-1 (RTD-1). *Bioorg. Med. Chem. Lett. 22*, 2823−2826.
(26) Gould, A., Li, Y. L., Majumder, S., Garcia, A. E., Carlsson, P., Shekhtman, A., and Camarero, J. A. (2012) Recombinant production of rhesus θ-defensin-1 (RTD-1) using a bacterial expression system. *Mol. Biosyst. 8*, 1359−1365.
(27) Sarin, V. K., Kent, S. B. H., Tam, J. P., and Merrifield, R. B. (1981) Quantitative monitoring of solid-phase peptide-synthesis by the ninhydrin reaction. *Anal. Biochem. 117*, 147−157.
(28) Dawson, P. E., Muir, T. W., Clark-Lewis, I., and Kent, S. B. (1994) Synthesis of proteins by native chemical ligation. *Science 266*, 776−779.
(29) Conibear, A. C., Daly, N. L., and Craik, D. J. (2012) Quantification of small cyclic disulfide-rich peptides. *Biopolymers 98*, 518−524.
(30) Marion, D., and Wüthrich, K. (1983) Application of phase sensitive two-dimensional correlated spectroscopy (COSY) for measurements of ^{1}H-^{1}H spin-spin coupling constants in proteins. *Biochem. Biophys. Res. Commun. 113*, 967−974.
(31) Hwang, T. L., and Shaka, A. J. (1995) Water suppression that works: Excitation sculpting using arbitrary wave-forms and pulsed-field gradients. *J. Magn. Reson. 112*, 275−279.
(32) Braunschweiler, L., and Ernst, R. R. (1983) Coherence transfer by isotropic mixing: Application to proton correlation spectroscopy. *J. Magn. Reson. 53*, 521−528.
(33) Jeener, J., Meier, B. H., Bachmann, P., and Ernst, R. R. (1979) Investigation of exchange processes by two-dimensional NMR spectroscopy. *J. Chem. Phys. 71*, 4546−4553.
(34) Rance, M., Sørensen, O. W., Bodenhausen, G., Wagner, G., Ernst, R. R., and Wüthrich, K. (1983) Improved spectral resolution in COSY ^{1}H NMR spectra of proteins via double quantum filtering. *Biochem. Biophys. Res. Commun. 117*, 479−485.
(35) Griesinger, C., Sørensen, O. W., and Ernst, R. R. (1987) Practical aspects of the e.COSY technique, measurement of scalar spin-spin coupling constants in peptides. *J. Magn. Reson. 75*, 474−492.
(36) Palmer, A. G., Cavanagh, J., Wright, P. E., and Rance, M. (1991) Sensitivity improvement in proton-detected 2-dimensional hetero-nuclear correlation NMR-spectroscopy. *J. Magn. Reson. 93*, 151−170.
(37) Wagner, G. (1990) NMR investigations of protein structure. *Prog. NMR Spectrosc. 22*, 101−139.
(38) Vranken, W. F., Boucher, W., Stevens, T. J., Fogh, R. H., Pajon, A., Llinas, P., Ulrich, E. L., Markley, J. L., Ionides, J., and Laue, E. D. (2005) The CCPN data model for NMR spectroscopy: Development of a software pipeline. *Proteins 59*, 687−696.
(39) Wüthrich, K. (1986) *NMR of proteins and nucleic acids*, Wiley-Interscience, New York.
(40) Cierpicki, T., and Otlewski, J. (2001) Amide proton temperature coefficients as hydrogen bond indicators in proteins. *J. Biomol. NMR 21*, 249−261.
(41) Wu, D. H., Chen, A. D., and Johnson, C. S. (1995) An improved diffusion-ordered spectroscopy experiment incorporating bipolar-gradient pulses. *J. Magn. Reson. 115*, 260−264.
(42) Altieri, A. S., Hinton, D. P., and Byrd, R. A. (1995) Association of biomolecular systems via pulsed field gradient NMR self-diffusion measurements. *J. Am. Chem. Soc. 117*, 7566−7567.
(43) Wilkins, D. K., Grimshaw, S. B., Receveur, V., Dobson, C. M., Jones, J. A., and Smith, L. J. (1999) Hydrodynamic radii of native and denatured proteins measured by pulse field gradient NMR techniques. *Biochemistry 38*, 16424−16431.
(44) Guntert, P., Mumenthaler, C., and Wüthrich, K. (1997) Torsion angle dynamics for NMR structure calculation with the new program DYANA. *J. Mol. Biol. 273*, 283−298.
(45) Cornilescu, G., Delaglio, F., and Bax, A. (1999) Protein backbone angle restraints from searching a database for chemical shift and sequence homology. *J. Biomol. NMR 13*, 289−302.
(46) Shen, Y., Delaglio, F., Cornilescu, G., and Bax, A. (2009) TALOS plus: A hybrid method for predicting protein backbone torsion angles from NMR chemical shifts. *J. Biomol. NMR 44*, 213−223.
(47) Nederveen, A. J., Doreleijers, J. F., Vranken, W., Miller, Z., Spronk, C., Nabuurs, S. B., Guntert, P., Livny, M., Markley, J. L., Nilges, M., Ulrich, E. L., Kaptein, R., and Bonvin, A. (2005) Recoord: A recalculated coordinate database of 500+ proteins from the PDB using restraints from the BioMagResBank. *Proteins 59*, 662−672.
(48) Brunger, A. T., Adams, P. D., Clore, G. M., DeLano, W. L., Gros, P., Grosse-Kunstleve, R. W., Jiang, J. S., Kuszewski, J., Nilges, M., Pannu, N. S., Read, R. J., Rice, L. M., Simonson, T., and Warren, G. L. (1998) Crystallography & NMR system: A new software suite for macromolecular structure determination. *Acta Crystallogr. D54*, 905−921.
(49) Dominguez, C., Boelens, R., and Bonvin, A. (2003) Haddock: A protein-protein docking approach based on biochemical or biophysical information. *J. Am. Chem. Soc. 125*, 1731−1737.
(50) Linge, J. P., and Nilges, M. (1999) Influence of non-bonded parameters on the quality of NMR structures: A new force field for NMR structure calculation. *J. Biomol. NMR 13*, 51−59.
(51) Chen, V. B., Arendall, W. B., Headd, J. J., Keedy, D. A., Immormino, R. M., Kapral, G. J., Murray, L. W., Richardson, J. S., and Richardson, D. C. (2010) Molprobity: All-atom structure validation for macromolecular crystallography. *Acta Crystallogr. D66*, 12−21.
(52) Koradi, R., Billeter, M., and Wüthrich, K. (1996) Molmol: A program for display and analysis of macromolecular structures. *J. Mol. Graphics 14*, 29−32.
(53) Wishart, D. S., Bigam, C. G., Holm, A., Hodges, R. S., and Sykes, B. D. (1995) ^{1}H, ^{13}C and ^{15}N random coil NMR chemical shifts of the common amino acids. I. Investigations of nearest-neighbor effects. *J. Biomol. NMR 5*, 67−81.
(54) Craik, D. J., Kumar, A., and Levy, G. C. (1983) Moldyn: A generalized program for the evaluation of molecular-dynamics models using nuclear magnetic-resonance spin-relaxation data. *J. Chem. Inf. Comput. Sci. 23*, 30−38.
(55) Jarvis, J. A., and Craik, D. J. (1995) C-13 NMR relaxation studies of molecular-motion in peptide-fragments from human transthyretin. *J. Magn. Reson., Ser. B 107*, 95−106.
(56) Berjanskii, M. V., and Wishart, D. S. (2005) A simple method to predict protein flexibility using secondary chemical shifts. *J. Am. Chem. Soc. 127*, 14970−14971.
(57) Camarero, J. A., and Muir, T. W. (1997) Chemoselective backbone cyclization of unprotected peptides. *Chem. Commun.*, 1369−1370.
(58) Camarero, J. A., Pavel, J., and Muir, T. W. (1998) Chemical synthesis of a circular protein domain: Evidence for folding-assisted cyclization. *Angew. Chem., Int. Ed. 37*, 347−349.
(59) Jaulent, A. M., Brauer, A. B., Matthews, S. J., and Leatherbarrow, R. J. (2005) Solution structure of a novel C_2-symmetrical bifunctional bicyclic inhibitor based on SFTI-1. *J. Biomol. NMR 33*, 57−62.
(60) Azimi, I., Wong, J. W. H., and Hogg, P. J. (2011) Control of mature protein function by allosteric disulfide bonds. *Antioxid. Redox Signaling 14*, 113−126.
(61) Selsted, M. E., and Ouellette, A. J. (2005) Mammalian defensins in the antimicrobial immune response. *Nat. Immunol. 6*, 551−557.